The Journal of Neuroscience, September 1, 2001, *21*(17):6673–6686

Multiple Amidated Neuropeptides Are Required for Normal Circadian Locomotor Rhythms in *Drosophila*

Paul H. Taghert,[1] Randall S. Hewes,[1] Jae H. Park,[2,3] Martha A. O'Brien,[1] Mei Han,[1] and Molly E. Peck[1]

[1]Department of Anatomy and Neurobiology, Washington University School of Medicine, St. Louis, Missouri 63110, [2]Department of Biology, Brandeis University, Waltham, Massachusetts 02454, and [3]Department of Biochemistry, Cellular and Molecular Biology, University of Tennessee, Knoxville, Tennessee 37996

In *Drosophila*, the amidated neuropeptide pigment dispersing factor (PDF) is expressed by the ventral subset of lateral pacemaker neurons and is required for circadian locomotor rhythms. Residual rhythmicity in *pdf* mutants likely reflects the activity of other neurotransmitters. We asked whether other neuropeptides contribute to such auxiliary mechanisms. We used the *gal4*/*UAS* system to create mosaics for the neuropeptide amidating enzyme PHM; amidation is a highly specific and widespread modification of secretory peptides in *Drosophila*. Three different *gal4* drivers restricted PHM expression to different numbers of peptidergic neurons. These mosaics displayed aberrant locomotor rhythms to degrees that paralleled the apparent complexity of the spatial patterns. Certain PHM mosaics were less rhythmic than *pdf* mutants and as severe as *per* mutants. Additional *gal4* elements were added to the weakly rhythmic PHM mosaics. Although adding *pdf-gal4* provided only partial improvement, adding the widely expressed *tim-gal4* largely restored rhythmicity. These results indicate that, in *Drosophila,* peptide amidation is required for neuropeptide regulation of behavior. They also support the hypothesis that multiple amidated neuropeptides, acting upstream, downstream, or in parallel to PDF, help organize daily locomotor rhythms.

Key words: circadian rhythms; Drosophila*; neuropeptide; amidation; PHM;* gal4*; PDF*

Relatively little is known about output signals used by circadian pacemaker neurons. In mammals, pacemaker neurons controlling daily locomotion are located in the suprachiasmatic nucleus (SCN), which contains several thousand cells that present several transmitter phenotypes (Silver et al., 1999). The SCN may release diffusible substances to influence behavioral rhythms (Silver et al., 1996), although the identity of such substances remains unknown. In *Drosophila*, the lateral neurons (LNs) are critical pacemakers regulating daily locomotor rhythms. A ventral subset of LNs (LN-Vs) (Ewer et al., 1992) expresses the neuropeptide pigment dispersing factor (PDF) (Helfrich-Förster, 1995) that is highly related to crustacean pigment dispersing hormone (PDH). Loss of PDF expression produces abnormal locomotor rhythms, and ablation of the PDF neurons produces a very similar phenotype (Renn et al., 1999). These genetic results confirm that LN-Vs are the principal circadian pacemaker neurons in *Drosophila* (cf. Frisch et al., 1994) and support the hypothesis that *pdf* encodes the principal circadian transmitter. However, *pdf* mutant animals are still able to entrain (Renn et al., 1999), and by quantitative measures, their free-running phenotype is less severe than that of *disco* mutants (Dushay et al., 1989; Helfrich-Förster, 1998). In *disco* mutants, the brain lacks many neurons, including all LNs. Together, these features suggest that additional transmitters are needed to produce normal circadian locomotor rhythms.

To identify such transmitters, we manipulated the biosynthesis of neuropeptides by creating genetic mosaics. In particular, we studied the behavioral consequences of cell-specific deficiencies in C-terminal peptide α-amidation (for review, see Eipper et al., 1993). In vertebrates, >50% of known neuropeptides are amidated; in *Drosophila*, >90%, including PDF, are amidated (Hewes and Taghert, 2001). α-Amidation is a highly specific modification for secretory peptides, and the two enzymes catalyzing amidation (called PHM and PAL) are found exclusively within luminal vesicular compartments (Eipper et al., 1993). In *Drosophila*, PHM is encoded by the *PHM* gene (Kolhekar et al., 1997). *PHM* mutant animals die as late embryos or young larvae; peptide amidation in both larval and adult stages requires PHM enzyme (Jiang et al., 2000).

The present experimental design had three requirements. The first was to restore sufficient PHM activity to *PHM* mutant animals to prevent death and so permit the testing of adult behavior. For this, we used the *gal4* technique (Brand and Perrimon, 1993). The second was to limit the scope of restored PHM activity compared with its normal patterns and/or levels. For this, we chose *gal4* lines that featured differing numbers of peptidergic neurons in their expression patterns. The third requirement was

Received April 11, 2001; revised June 13, 2001; accepted June 20, 2001.

This work was supported by National Institutes of Health Grants NS-21749 to P.H.T. and GM-33205 to Jeff Hall (Brandeis University, Waltham, MA), National Research Service Award MH11946 to J.H.P., National Science Foundation Grant IBN 97–30003 to P.H.T., and the University of Tennessee New Investigator Supporting Program (J.H.P.). We thank Ning Jiang and Marie Roberts for assistance in creating UAS-*PHM* transgenic animals and Pam Vanderzalt for assistance with behavioral experiments. We thank Jeff Hall, in whose laboratory preliminary behavioral experiments were performed. We thank Andrea Brand for the pUAST vector and Kalpana White, Maki Kaneko, Jeff Hall, Sarah Smolik, Gabrielle Boulianne, the Bloomington Stock Center, and the Berkeley *Drosophila* Genome Project for *Drosophila* stocks. We thank Michael O'Connor for allowing us to use the stock P{w^+, UAS-*dFMRFa*}. We thank Kalpana White and Gabrielle Boulianne for personal communications and Russ Van Gelder, Joel Levine, and Jeff Hall for helpful discussions and for their comments on a draft of this manuscript.

Correspondence should be addressed to Dr. Paul H. Taghert, Box 8108, Department of Anatomy and Neurobiology, Washington University School of Medicine, 660 South Euclid Avenue, St. Louis, MO 63110. E-mail: taghertp@thalamus.wustl.edu.

R. S. Hewes' present address: Department of Zoology, University of Oklahoma, 730 Van Vleet Oval, Norman, OK 73019.

J. H. Park's present address: Department of Biochemistry, Cellular and Molecular Biology, University of Tennessee, Knoxville, TN 37996.

M. A. O'Brien's present address: Promega Corporation, 2800 Woods Hollow Road, Madison WI 53711.

Table 1. Properties of the *gal4* lines used in the behavioral experiments

Name	Position (chromosome)/ nearest gene	Expression pattern	Reference
c929	39CD(II)/CG8669	Secretory cells; many tissues	1, 2
36Y	85C(III)/CG11033	Secretory cells; many tissues	1
386Y	97D(III)/CG6438	Secretory cells; many tissues	3
Appl 3GK	III/5, n.d.	CNS only; low in optic lobes; broadly in central brain	4
D42	III/n.d.	~200 CNS neurons, including motorneurons	5
tim(#16)	III/n.d.	Broadly within CNS	3, 6
tim(#67)	III/n.d.	n.d.	3
pdf (M)	X/n.d.	Similar to *pdf*	7
pdf (N)	X/n.d.	Similar to *pdf*	7

n.d., Not determined. 1, O'Brien and Taghert, 1998; 2, Hewes et al., 2000; 3, this work; 4, K. White, personal communication; 5, G. Boulianne, personal communication; 6, Kaneko and Hall, 2000; 7, Park et al., 2000.

to ensure that PHM activity in these mosaic animals was restored within PDF LN-Vs to ask whether neuropeptides other than PDF participate in the regulation of daily locomotion. For this, we analyzed combinations of *gal4* elements that included *pdf-gal4* (Park et al., 2000). The results demonstrate that (1) the normal display of daily locomotor rhythms requires the participation of amidated peptide transmitters, and (2) amidated neuropeptides in addition to PDF are required for this behavioral regulation.

MATERIALS AND METHODS

Genetic strains. The two alleles of *PHM* used in these studies were described by Jiang et al. (2000). P{*lacW*}k[07623] is a P-element insertion within the first exon of *PHM*; here we refer to it as PHM^{01}. PHM^{P29} contains a ~1.3 kb deletion generated by mobilizing the k[07623] element; here we refer to it as PHM^{02}. PHM^{01} is a strong hypomorphic allele, whereas PHM^{02} appears to be a null. Because PHM^{02} also deletes sequences belonging to a neighboring gene (Jiang et al., 2000), we analyzed the *trans*-heterozygote combination PHM^{01}/PHM^{02}. Deficiency stocks were obtained from the Bloomington Stock Center (Indiana University, Bloomington, IN). *P{gal4}* lines are summarized in Table 1. The *c929-gal4* insertion (at 39C4 of the second chromosome) (Hewes et al., 2000) was recombined onto the chromosome bearing the PHM^{01} allele. Second chromosome mutations were balanced by *In(2LR)O*, *Cy*, y^+; third chromosome mutations were balanced by *In(3LR)TM3*, *Sb*. Canton-S was used for a wild-type (WT) strain.

Molecular biology. Standard molecular methods were used (Maniatis et al., 1982). A UAS-*PHM* construct was assembled by isolating the *Eco*RI-*Kpn*I fragment of *PHM* cDNA #1 (Kolhekar et al., 1997), blunt-ending the *Kpn*I site, then ligating the insert into the CaSpeR-based vector pP{UAST} at the *Eco*RI and *Not*I sites. Several independent germ line transformants were made and recovered by standard procedures (Benveniste and Taghert, 1999). Briefly, DNAs were purified by Qiagen miniprep protocols, according to the manufacturer's recommendations, and injected at a concentration of ~750 ng/ml into embryos homozygous for the element *P{(Δ2–3)99B}* that is a source of transposase activity. Backcrosses of positive transformants to balanced stocks that contained dominant markers were used to identify insertion chromosomes. Southern blot analyses were used to determine *P*-element copy number. Western blots were used to evaluate basal and induced levels of PHM. In all studies reported here, we used a single-copy, homozygous-viable, second chromosome insertion (C1A) that was recombined onto the chromosome bearing the PHM^{02} allele.

Single-fly PCR. To confirm the genotype of recombinants, we used the procedure of Gloor et al. (1993). Two pairs of oligonucleotides were used in single or multiplex PCR to determine the presence of *PHM* mutant alleles, as described by Jiang et al. (2000).

Mapping P-element insertion positions. We used methods described by the Berkeley *Drosophila* Genome Project (BDGP – http://www.fruitfly.org/about/methods/inverse.pcr.html) to map the position of the P{w^+, *gal4*}*386Y* insertion. It is found at bp ~118,100 of GenBank sequence number AE003757. This position is within 320 bp of the 3′ end of *amontillado* (CG6438), which encodes the *Drosophila* homolog of the neuropeptide-processing enzyme PC2 (Siekhaus and Fuller, 1999); it is also within 1544 bp of the 5′ end of the neighboring gene CG6425. The position of the P{w^+, *gal4*}*36Y* insertion was determined by plasmid-rescue methods: a ~2 kb *Pst*I-flanking fragment was subcloned and sequenced. The insertion site lies at bp ~144,300 of GenBank sequence number AE003681, within the first intron of CG11033.

Immunocytochemistry. CNS and gut tissues were stained in whole mount using procedures similar to those described in Renn et al. (1999). Rabbit anti-dPHM was used at a 1:750 dilution (Kolhekar et al., 1997); guinea pig anti-PAP (this recognizes an non-PDF epitope on the proPDF precursor) (Renn et al., 1999) was used at 1:1000; rabbit anti-FMRFamide (Taghert and Schneider, 1990) was used at 1:2000; mouse anti-βGAL (Promega, Madison WI) was used at 1:1000. Secondary antibodies (Jackson ImmunoResearch, West Grove, PA) conjugated with Cy3 or Alexa 468 were used at 1:200 or 1:500 dilutions. Tissues were cleared in glycerol, mounted in Vectashield (Vector Laboratories, Burlingame, CA), and examined with an Olympus confocal microscope and Fluoview software or with a Zeiss Axioplan microscope fitted with a Spot CCD camera (Diagnostics Instruments, Sterling Heights, MI). Confocal images were assembled in Adobe Photoshop. Spot camera images were used for quantification of immunosignals. In Adobe Photoshop, histogram values of fluorescence intensity from single cell bodies (less than from equivalent background areas immediately adjacent) were acquired for both anti-PHM and anti-PAP signals.

Behavioral analysis. Locomotor activity rhythms of 1- to 5-d-old adult males were monitored at 25°C as described in Hamblen et al. (1986, 1998). Locomotor performance was measured using analytic software provided by the Brandeis Rhythm Package (http://hawk.bcm.tmc.edu/). We first monitored behavior over 7–8 d in 12 hr light/dark (LD) conditions; free-running activity was then monitored in constant darkness (DD) for a further 9–10 d. The number of activity events was recorded per half-hour bin, and average numbers of activity events per bin, per fly were calculated (cf. Hamblen-Coyle et al., 1989). χ^2 periodogram analyses (Sokolove and Bushell, 1978) identified animals displaying behavioral rhythmicity with the following thresholds: power ≥ 10 and width ≥ 2.0 (cf. Ewer et al., 1992; Renn et al., 1999). For more sensitive determinations of free-running periodicities, the activities were subjected to a low-pass digital filter (Dowse and Ringo, 1987), then analyzed by Maximum Entropy Spectral Analysis (MESA) (cf. Dowse and Ringo, 1987; Hamblen-Coyle et al., 1989). Subsequently, a MESA-based signal-to-noise ratio (SNR) for each fly was computed (Dowse and Ringo, 1987) and averaged per genotype. SNR averages were $\log_{10}$-transformed; one-way ANOVAs and *post hoc* tests (Dunnett's test; all versus control) were performed with InStat (GraphPad, San Diego, CA). All behavioral data studying genotypes that have already been described (e.g., per^{01}) represent results not previously published.

RESULTS

gal4 patterns

The *36Y-gal4* element is inserted within CG11033, which encodes a protein that contains PHD domain found in a class of transcription factors (Aasland et al., 1995). The *36Y-gal4* enhancer pattern has not yet been associated with a specific gene. Aspects of the larval *36Y-gal4* pattern were described by O'Brien and Taghert (1998). Using UAS-*lacZ* expression as a reporter, *36Y-gal4* neural expression was the most restricted of any *gal4* tested in these experiments, after *pdf-gal4*. In the adult ($n = 20$; data not shown), UAS-*lacZ* was limited to ~30 neurons scattered in the central brain and several cells within the optic lobes that defined a parallel array. Many of the neurons appear to be peptidergic by

Table 2. Rescue of *PHM* lethality produced by different *gal4*/*UAS-PHM* combinations

Potential rescued *PHM* mosaic (i.e., Cy^+)		# Cy^+	# Cy^-	% of Cy^+ expected
y w; PHM^{01}/UAS-*PHM*, PHM^{02}; *36Y-gal4*	/+	80	138	110
y w; *c929-gal4*, PHM^{01}/UAS-*PHM*, PHM^{02};		110	381	67
y w; PHM^{01}/UAS-*PHM*, PHM^{02}; *386Y-gal4*	/+	32	112	67
y w; *c929-gal4*, PHM^{01}/UAS-*PHM*, PHM^{02}; *36Y-gal4*	/+	28	51	107
y w; *c929-gal4*, PHM^{01}/UAS-*PHM*, PHM^{02}; *D42-gal4*	/+	21	74	68
y w; *c929-gal4*, PHM^{01}/UAS-*PHM*, PHM^{02}; *Appl*(3GK)	/+	37	59	116
y w; *c929-gal4*, PHM^{01}/UAS-*PHM*, PHM^{02}; *tim(#16)-gal4*	/+	76	169	93
y w; PHM^{01}/UAS-*PHM*, PHM^{02}; *tim(#16)-gal4*	/+	0	85	0
y w; PHM^{01}/UAS-*PHM*, PHM^{02}; *tim(#67)-gal4*	/+	0	77	0

Cy^+, The number of rescued *PHM* mutant animals (adults not displaying the marker for the Balancer chromosome and therefore *trans*-heterozygous for the two *PHM* alleles); # Cy^-, the number of heterozygous *PHM* mutant animals (adults displaying the marker for the Balancer chromosome, *CyO*); % of Cy^+ expected, percentage of *PHM* mutant animals observed and/or expected.

cell body position and by double antibody staining (data not shown), including a small number of neurons in the vicinity of the PDF-expressing LN pacemakers. *36Y-gal4* expression included strong staining in two peritracheal endocrine cells, called PMa and PMb (O'Brien and Taghert, 1998). PMa is the probable Inka cell homologue (Zitnan et al., 1996). *36Y-gal4* expression was also prominent in ring gland, salivary glands, fat body, epidermis, and hindgut ($n = 20$).

The *c929-gal4* element is inserted in the *cryptocephal* gene (*crc*, CG8669, *dATF-4*) (Hewes et al., 2000); however, its expression pattern does not match that of *crc*, but rather matches that of an adjacent gene (R. S. Hewes and P. H. Taghert, unpublished observations). This pattern ($n > 30$; data not shown) included ~100 neurons in the CNS. All (or nearly all) *c*929-*gal4* positive neurons are peptidergic, as judged by double immunostaining with antibodies against diverse neuropeptides and neuropeptide biosynthetic enzymes (R. S. Hewes and P. H. Taghert, unpublished observations). In particular, the *c929-gal4* pattern precisely overlapped that of strong PHM immunosignals, with very few exceptions. In adults, the *c929-gal4* pattern included a set of neurons similar to that of *36Y-gal4*, but typically displayed more cells per area, and the cells were often more densely stained (e.g., the LN area). *c929-gal4* was expressed in the peritracheal PMa endocrine cell, but not in cell PMb (cf. O'Brien and Taghert, 1998). The neurilemma of the brain was βGAL-positive in *c929 gal4* animals; the pattern also included heterogenous expression in a variety of other tissues, including ring gland cells, epidermis, the gut endocrine system, salivary glands, and fat body ($n > 20$).

We located the *386Y-gal4* element just 3′ to *amontillado* (CG6438), which is the *Drosophila* homolog of the proprotein processing enzyme PC2 (Siekhaus and Fuller, 1999). As tested with UAS-*lacZ*, the *386Y-gal4* expression pattern was broad and included numerous peptidergic neurons in the CNS ($n = 15$; data not shown) and secretory cells in the periphery ($n = 4$). The number of *386Y*-positive cells was considerably greater than that of either *36Y*- or *c929-gal4* patterns. The *386Y-gal4* pattern included many neurons in the vicinity of LNs, numerous Kenyon cells, as well as other prominent peptidergic neurons (data not shown). In larval stages, the PDF LN-Vs (usually three or four per hemisphere) co-expressed βGAL ($n = 5$); in adults, only the large LN-Vs co-expressed βGAL ($n = 4$; data not shown). Outside the CNS, *386Y-gal4* drove heterogeneous expression in numerous tissues; most of this expression was correlated with secretory cell activity (e.g., in gut, in peritracheal cells, and in neurosecretory neurons of the PNS; data not shown).

The *pdf*(M) and *pdf*(N)-*gal4* elements are independent insertion lines of the same transgene. They produced βGAL patterns that were largely comparable with each other and with the pattern described by Park et al. (2000), namely, restriction to PDF-expressing CNS cells, including strong expression in both large and small LN-Vs, in two to four tritocerebral cells in young imagos and in approximately six abdominal ganglion gut efferents ($n = 4$ each). The cell bodies of small LN-Vs normally stain weakly for PDF, compared with those of large LN-Vs. However, the strength of reporter gene expression in small LN-Vs appeared very strong in both lines and similar to that of the large LN-Vs. Ectopic *lacZ* expression was seen in approximately eight neurons of the subesophaegal region in the (M) line and in two small neurons of the protocerebrum in the (N) line (data not shown).

The *tim(#16)-gal4* driver produced a very broad and strong expression pattern throughout the adult brain ($n = 4$) (cf. Kaneko and Hall, 2000). Its expression outside the CNS was not studied (but see Kaneko and Hall, 2000). *Appl*(3GK)-*gal4* produced a strong and diverse pattern throughout the adult brain that included numerous cells in all brain regions ($n = 4$); the extent of the pattern was comparable with that of *386Y-gal4*, but appeared less than that of *tim-gal4. c155-gal4* (Lin and Goodman, 1994) produced a weak level of expression throughout many brain regions and moderate expression in several large neurons of the subesophageal region ($n = 8$).

Reverting *PHM* lethality with the *gal4*/*UAS* system

We asked whether any of seven different *gal4* drivers could produce sufficient PHM activity in a *PHM* mutant background to revert the early lethality associated with the *PHM* phenotype (Jiang et al., 2000). Table 2 presents the degree to which these genetic combinations could rescue animals *trans*-heterozygous for the two alleles, PHM^{01} and PHM^{02}. Neither of two *tim-gal4* lines (#16 or #67) was able to drive UAS-*PHM*-mediated rescue *PHM* mutant animals, whereas *c929-gal4* and *386Y-gal4* provided partial rescue (each ~67% of expected). *36Y-gal4* provided a strong measure of rescue in driving *UAS-PHM*. Combining *36Y-gal4* and *c929-gal4* drivers produced a measure of rescue comparable with that of *36Y-gal4* alone. Rescued adult animals of all genotypes that were tested survived the 18 d period of the behavioral assay as well as did the wild-type stock. In the following, we simplify the

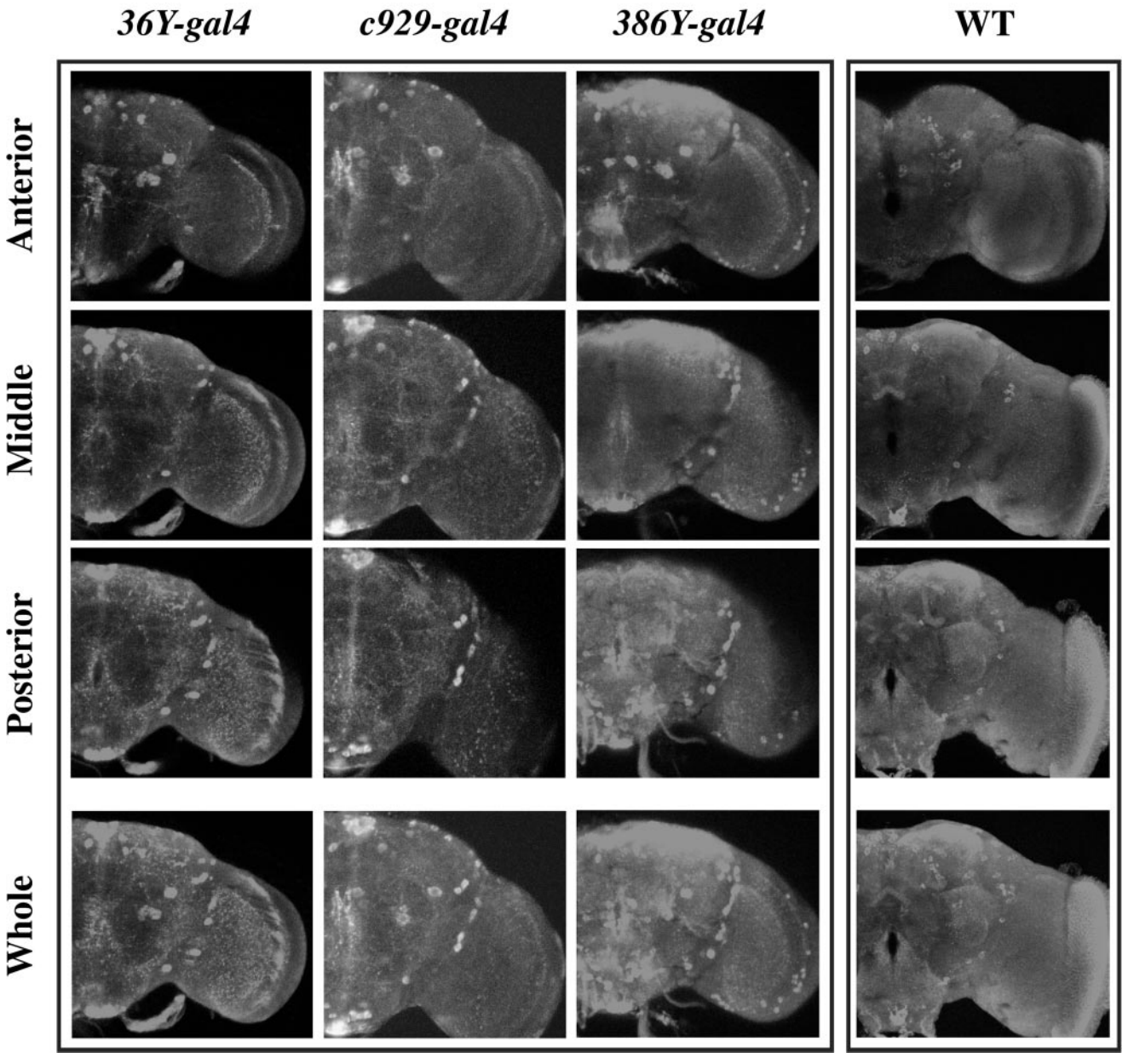

Figure 1. Expression of PHM immunostaining driven by different *gal4* drivers in a *PHM* null background. Each column displays a three-part series of confocal images from a single adult male brain of the genotype indicated. The *bottom panels* (*Whole*) represent overlays of the three-volume sections and depict nearly the entire brain thickness. The three separate scans display *anterior*, *middle*, and *posterior* sections of the brain. For the wild-type (*WT*) brain, *36Y*-rescued animals, and *c929*-rescued animals, section depths were 66, 60, and 60 μm, respectively. For *386Y-gal4*-rescued animals, section depths were 72, 60, and 60 μm, respectively.

text by describing the behavior of *UAS-PHM*-rescued *PHM* mutant flies with reference only to the *gal-4* driver(s) that was used (e.g., *36Y-gal4*-rescued animals).

gal4 restricts PHM expression

To visualize the restriction of UAS-*PHM* by the different *gal4* drivers in a *PHM* mutant background, we stained the brains of rescued adult males (1–10 d old) for PHM immunosignals and compared them with wild-type tissues. Wild-type brains display widespread and heterogeneous PHM staining ($n = 15$) (Fig. 1). PHM-like immunoreactivity is seen in several large cell bodies, including some in the lateral and dorsal protocerebrum, in subesophageal neuromeres, and among Kenyon cells. It also highlights several organized neuropils, like the lobes of the Mushroom bodies and several sections of the Fan-Shaped body, and appears strongly in dorsal protocerebral neuropil and neuropil surrounding the esophageal foramen. *36Y-gal4*-rescued animals ($n = 8$) displayed PHM immunosignals in several identifiable peptidergic neurons [e.g., MP1 and MP2 neurons (O'Brien et al., 1991)] on a generally low background of staining (Figs. 1, 2). With *c929-gal4* ($n = 6$), there was a very similar pattern, but with several additional cell bodies in the dorsal protocerebrum, in the LN cell body region, and in the subesophageal neuromeres. There were also a greater number of stained processes (Fig. 1). The pattern of *c929-gal4*/UAS-*PHM* expression differed slightly from that of *c929-gal4*/UAS-*lacZ*; the latter included numerous cells of the neurilemma, but this feature was not apparent with PHM expres-

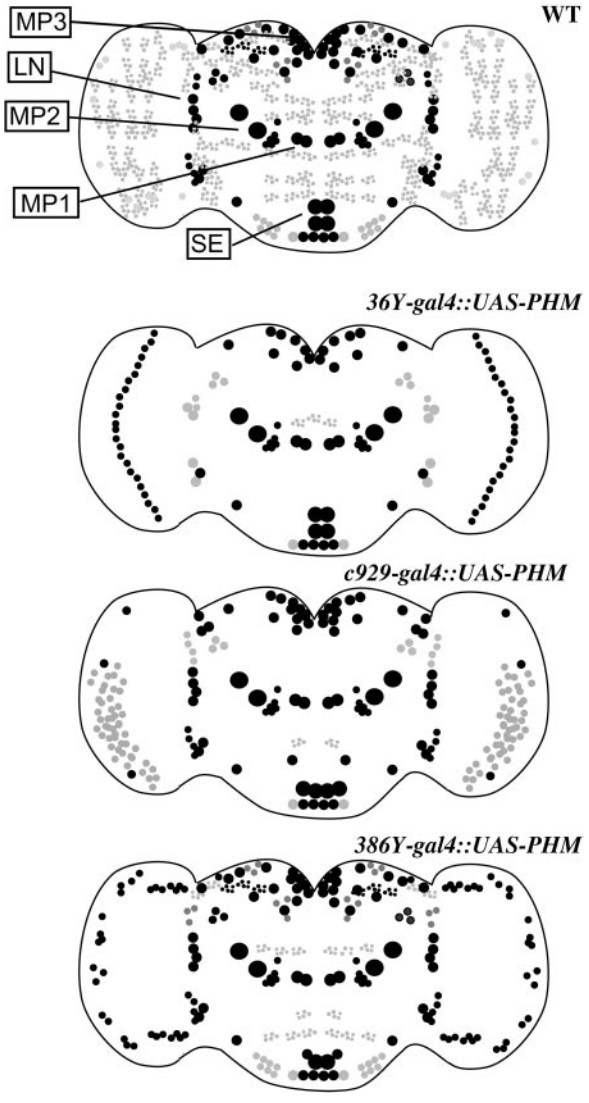

Figure 2. Schematic diagrams of the staining patterns displayed in Figure 1. The genotypes are indicated to the *left* of each panel. The sizes and positions of various cell bodies are approximate. *Black* indicates strong staining; *gray* indicates weak to moderate staining. Many cell types included in these patterns appeared similar; double antibody staining experiments confirmed that many cellular elements are shared (see text for further details). *MP1*, *MP2*, *MP3*, *LN*, and *SE* indicate prominent peptidergic cell groups; most preparations included one or more representatives of each group.

sion. Finally, *386Y-gal4*-rescued animals ($n = 8$) displayed a much broader level of staining throughout the brain, including numerous strongly stained cells in the LN cell body region and throughout the dorsal protocerebrum (Fig. 1). These animals also displayed a greater "background" level of immunostaining, suggesting a general low level of expression in many scattered cells. Figure 2 presents drawings to schematize these generalized cellular patterns.

We also asked whether the PDF neurons of the brain of rescued animals were specifically included in any of the above three *gal4* patterns: *36Y*, *c929*, or *386Y*. We performed double antibody labeling on these genotypes for PHM and for identified LN-V neurons by anti-proPDF staining. *36Y-gal4* displayed weak PHM expression in one or two large PDF LN-Vs, but not in the small LN-Vs (data not shown). *c929-gal4* and *386Y-gal4* displayed expression patterns that were greater than *36Y-gal4* and similar to each other; they contained bright PHM immunolabeling in all of the large PDF LN-Vs and the tritocerebral cells, but in not the small LN-Vs ($n = 12$). Figure 3 shows an example of PHM immunostaining in LN-Vs in a *PHM* mutant rescued by expression of *PHM* driven by two *gal4* elements, *c929-gal4* and *386Y-gal4* ($n = 4$). Even together, these two elements do not generate detectable PHM immunosignals in the small LN-Vs of the adult.

PHM expression in PDF neurons

We first studied PHM immunostaining of PDF-expressing neuronal cell bodies in wild-type animals. PHM immunosignals include high level expression in ~100 brain neurons and a low (perhaps ubiquitous) level of staining in most other cells. We measured the ratio of immunosignal strength (proPDF to PHM) in the three different PDF neurons of the brain, i.e., large LN-Vs, small LN-Vs, and tritocerebral cells in <1-d-old adult male brain hemispheres ($n = 10$). Although the large LN-Vs and the tritocerebral cells contained detectable PHM immunosignals, the small LN-Vs had little to none (Table 3). We next tested the ability of small LN-Vs to accumulate PHM and display PHM immunosignals. We crossed *pdf* (M) and (N) *gal4* lines to UAS-*PHM* in a wild-type background. In five of five adult brains from each cross, anti-PHM antibody stained the cell bodies (weakly) and processes (moderately) of the small LN-Vs (data not shown).

The lack of PHM immunosignals in wild-type small LN-Vs prompted us to test for the presence of functional amidating activity in those cells. The anti-PDH (crab PDF) antibody that we use does not discriminate between amidated and nonamidated forms of the peptide; *PHM* mutant animals are stained normally by this antibody before they die (M. Han and P. H. Taghert, unpublished observations). However, the PT-2 antibody against FMRFamide-like peptides discriminates strongly between amidated and unamidated peptides (Jiang et al., 2000). Therefore, we misexpressed *dFMRFa* transcripts in small LN-Vs by crossing UAS-*dFMRFa* flies to each of three *pdf-gal4* lines [Bmr(J), M and N] in a wild-type background. We stained resultant larval and adult brains with anti-FMRFa antibody. In five of five specimens of both stages from each cross, both small and large LN-Vs were FMRFamide-immunopositive in both cell bodies and processes (data not shown); large LN-Vs were strongly stained and small LN-Vs were weakly or moderately stained. In summary, the small LN-Vs of WT flies do not contain detectable PHM immunosignals, but they accumulate over-expressed PHM, and they possess endogenous PHM-like amidating activity.

Locomotor behavior under cycling conditions

We compared the behavior of the *PHM* mosaic flies with that of three genotypes: (1) wild type (WT), (2) per^{01}, and (3) pdf^{01}. We present the analysis in three formats: as tabulated data in Table 4, as average-activity histograms (e.g., Fig. 4), and as distributions of SNR values for individuals under constant conditions (Fig. 5). The SNR method is described in Materials and Methods. The range of SNR values for WT flies is shown in Figure 5.

Under 12 hr LD cycles, WT males produced two peaks of activity (cf. Hamblen-Coyle et al., 1992). The morning peak was maximal around lights on and anticipated that transition; the evening peak was maximal around lights off and also anticipated that transition (Fig. 4*E*). In contrast, per^{01} flies displayed only transient peaks of activity that were coincident with the light/dark transitions and that showed no anticipatory or sustained nature (Fig. 4*A*) (cf. Wheeler et al., 1993). Finally, pdf^{01} flies displayed

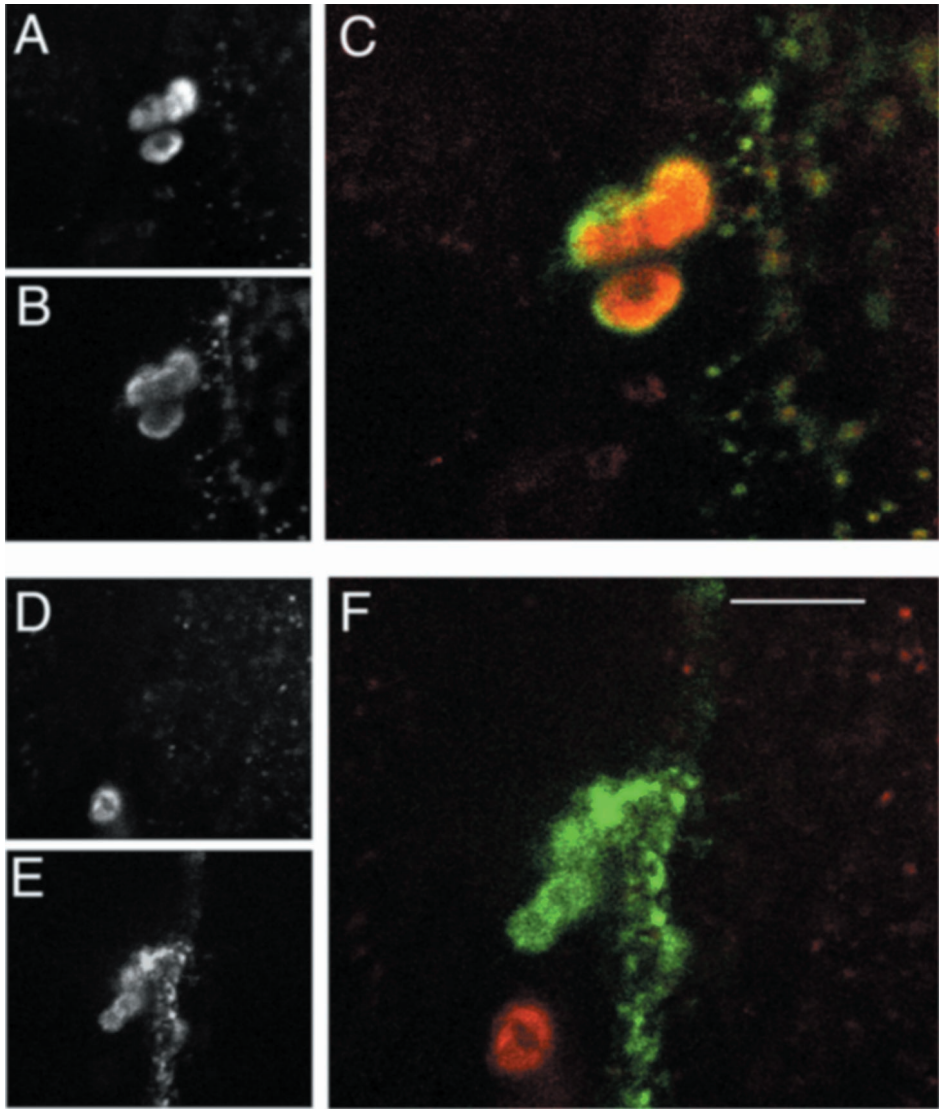

Figure 3. Double-immunostaining to identify PDF neurons included in *gal4* expression patterns. Confocal scans of the brain from an adult *PHM* mutant animal that was rescued by a combination of two *gal4* elements (*c929-gal4* and *386Y-gal4*) driving UAS-*PHM*. The tissue was stained for PHM and proPDF antibodies. Large LN-Vs are stained by both PHM (*A* and *C, red*) and proPDF (*B* and *C*, *green*). Small LN-Vs are only stained by proPDF antibodies (*E* and *F*, *green*), but not at all by PHM antibodies (*D* and *F*, *red*). Note another PHM-positive cell body in the vicinity of the small LN-Vs that is not proPDF-positive (*F*). These images were taken from different focal planes of the same specimen. Scale bar, 20 μm.

Table 3. Quantification of PHM and proPDF immunostaining in PDF neurons

Cell type	*n* (cells)	*N* (specimens)	proPDF (API)	PHM (API)	proPDF/PHM
Large LN-Vs	22	5	54.2 ± 5	4.3 ± 0.5	13
Small LN-Vs	17	5	25.5 ± 2	0.1 ± 0.4	212
Tritocerebral cells	4	3	27 ± 4	1.7 ± 1.8	15

Pixel intensity averages (API) after immunostaining of the three PDF cell types for PHM and for proPDF in brains of young adult males.

two peaks of activity. The morning peak lacked anticipation and was very narrow; the evening peak showed anticipation, was sustained, and was phase-advanced relative to that of WT (data not shown) (cf. Renn et al., 1999). The LD behavior of *36Y-gal4*-rescued flies (Fig. 4*B*) and *c929-gal4*-rescued flies (Fig. 4*C*) were similar. Both groups displayed two peaks of activity having normal peak time; locomotor levels accompanying these maxima were sustained, but in neither transgenic line did flies anticipate the morning lights-on transition. In *386Y-gal4*-rescued animals (Fig. 4*D*), both the morning and evening peaks appeared comparable with those of WT, and the morning peak displayed normal anticipation.

Locomotor behavior under constant conditions

Under conditions of DD, WT animals maintain daily rhythmicity with an activity profile that is temperature-dependent (Majercak et al., 1999). At 25°C, they display a single peak of activity, typically late in the subjective day. Table 4 presents the behavioral analysis of *PHM* mosaic animals for 7 d under constant conditions (DD days 3–9). Figure 4 presents average group activity plotted separately for DD days 1–2 and 3–9. The majority of WT flies (Table 4, line 1) remained rhythmic over the entire period (Fig. 4*J*,*O*); by periodogram analysis, 80% of individuals were rhythmic, and the population displayed an average SNR of 1.25. As previously reported (Wheeler et al., 1993), per^{01} animals

Table 4. Free-running behavior of different genotypes during days 3–9 under constant conditions

	Line	Genotype	N	tau	% R[a]	SNR	Sig.[b]	Events/bin
Standards	1	WT	107	23.7 ± 0.1 (91)	80	1.25 ± 0.1	**	17.4 ± 1
	2	*y w*; ; *pdf*^{01}	45	25.4 ± 2 (7)	16	0.50 ± 0.1	NS	12 ± 1
	3	*w*, *per*^{01}	29	23.0 ± 7.5 (2)	7	0.25 ± 0.2	**	15.3 ± 1
Controls	4	*y w*; + /UAS-*PHM*, ; *tim(#16)-gal4*	14	24.1 ± 0.1 (14)	100	0.81 ± 0.2	**	12.4 ± 2
	5	*y w*; *c929-gal4* /UAS-*PHM*	31	24.0 ± 0.1 (23)	75	1.16 ± 0.1	**	20.4 ± 1
	6	*y w*; *c929-gal4* /UAS-*PHM*, *PHM*^{02}	25	23.8 ± 0.1 (15)	61	0.95 ± 0.1	**	22.6 ± 1
	7	*y w*; *c929-gal4*, *PHM*^{01}/*y*$^{+}$, *CyO*	37	23.9 ± 0.1 (27)	73	0.68 ± 0.1	**	16.9 ± 1
	8	*y w*; *c929-gal4*, *PHM*^{01}/UAS-*PHM*	28	23.6 ± 0.1 (21)	100	1.11 ± 0.1	**	16.1 ± 1
	9	*y w*; *y*$^{+}$, *CyO*/UAS-*PHM*, *PHM*^{02}	50	23.9 ± 0.3 (41)	82	0.84 ± 0.1	**	16 ± 1
Single *gal4*s	10	*y w*; *PHM*^{01}/UAS-*PHM*, *PHM*^{02}; *386Y-gal4* / +	44	24.0 ± 0.4 (37)	77	0.95 ± 0.1	**	8.3 ± 1
	11	*y w*; *PHM*^{01}/UAS-*PHM*, *PHM*^{02}; *36Y-gal4* / +	49	25.8 ± 0.6 (3)	6	0.29 ± 0.1	**	6.3 ± 1
	12	*y w*; *c929-gal4*, *PHM*^{01}/UAS-*PHM*, *PHM*^{02}	54	35.7 (1)	3	0.48 ± 0.1	—	19.4 ± 1
Double *gal4*s	13	*y w*, *pdf-gal4*(N); *c929-gal4*, *PHM*^{01}/UAS-*PHM*, *PHM*^{02}	60	24.5 ± 0.1 (26)	43	0.55 ± 0.1	NS	17.5 ± 1
	14	*y w*, *pdf-gal4*(M); *c929-gal4*, *PHM*^{01}/UAS-*PHM*, *PHM*^{02}	82	23.8 ± 0.2 (18)	21	0.45 ± 0.1	NS	11.9 ± 1
	15	*y w*; *c929-gal4*, *PHM*^{01}/UAS-*PHM*, *PHM*^{02}; *36Y-gal4* / +	23	26.8 ± 3.3 (5)	30	0.42 ± 0.1	NS	11.8 ± 1
	16	*y w*; *c929-gal4*, *PHM*^{01}/UAS-*PHM*, *PHM*^{02}; *386Y-gal4* / +	81	23.7 ± 0.1 (66)	83	0.71 ± 0.1	**	13.1 ± 1
	17	*y w*; *c155-gal4*; *c929-gal4*, *PHM*^{01}/UAS-*PHM*, *PHM*^{02}	34	23.4 ± 0.1 (32)	72	0.48 ± 0.1	NS	11.4 ± 1
	18	*y w*, *c929-gal4*, *PHM*^{01}/UAS-*PHM*, *PHM*^{02}; *D42-gal4* / +	38	23.7 ± 0.3 (20)	53	0.35 ± 0.1	NS	10.5 ± 1
	19	*y w*; *c929-gal4*, *PHM*^{01}/UAS-*PHM*, *PHM*^{02}; *Appl* (3GK)-*gal4* / +	44	23.7 ± 0.4 (21)	48	0.42 ± 0.1	NS	14.6 ± 1
	20	*y w*; *c929-gal4*, *PHM*^{01}/UAS-*PHM*, *PHM*^{02}; *tim(#16)-gal4* / +	38	24.1 ± 0.1 (32)	84	0.76 ± 0.1	**	13.2 ± 1
	21	*y w*; *PHM*^{01}/UAS-*PHM*, *PHM*^{02}; *36Y-gal4* /*tim(#16)-gal4*	29	25.1 ± 0.3 (25)	84	0.89 ± 0.1	**	9.5 ± 1

tau, Period of the behavioral rhythm in hours. Dunnett's *post hoc* analysis, comparing all values to that of line 12 (*yw*; *c929-gal4*/UAS-*PHM*, *PHM*^{02}) produced the following conclusions: **, these stocks different at $p < 0.01$; NS, these stocks not significantly different. For testing, line 12 was compared separately to each of the four groups (Standards, Controls, Single *gal4*s, Double *gal4*s).

[a]Percentage rhythmic by χ-square periodogram analysis: $p \geq 10$ and $w \geq 2$.

[b]Significance: by ANOVA, SNR averages are significantly different ($p < 0.001$).

(Table 4, line 3) became largely arrhythmic in the first cycle of DD and remained so (Fig. 4*F*,*K*); only 7% of *per*^{01} animals in the current test were rhythmic during DD days 3–9, and their average SNR was 0.25. *pdf*^{01} animals (Table 4, line 2) remained rhythmic for DD days 1–2, but only 16% remained rhythmic over DD days 3–9 (data not shown) (cf. Renn et al., 1999); the population had an average SNR of 0.5.

36Y-gal4-rescued flies (Table 4, line 11) resembled *per*^{01}; they were very weakly rhythmic over DD days 1–2 (Fig. 4*G*) and DD days 3–9 (Fig. 4*L*). Six percent of these individuals were rhythmic, and the population displayed an average SNR of 0.29. *c929-gal4*-rescued flies (Table 4, line 12) were also poorly rhythmic during DD days 1–2 (Fig. 4*H*). During DD days 3–9, *c929-gal4*-rescued flies were only 3% rhythmic by periodogram (Fig. 4*M*), but the population displayed a higher SNR than *36Y-gal4*-rescued flies (0.49). In this regard they were more comparable with *pdf*^{01}. During the entire DD period, *386Y-gal4* flies displayed a pattern of activity approaching that of WT (Fig. 4*I*,*N*, Table 4, line 10).

The distribution of DD days 3–9 SNR averages permits evaluation of the behavior of individuals within a large population. As previously found (Renn et al., 1999), the range of SNR values for WT was 0.3 to >3; in contrast, that for *per*^{01} was clustered between 0.2 and 0.4 (Fig. 5*A*). The range of SNR values for *PHM* "mosaics" rescued by *36Y-gal4* resembled that of *per*^{01} (Fig. 5*B*). Values for *c929-gal4*-rescued flies were also low but included some nearing 0.8. *386Y-gal4*-rescued flies produced a broad range that largely overlapped that of WT.

The *PHM* mosaics were constructed by assembling several transgenes. To determine the degree to which the genetic background might influence the behavioral results, we measured locomotor rhythms in six additional control stocks (Table 4, lines 4–9). The latter five contained various subsets of these same transgenes, with or without a balancer chromosome (see Methods, Genetic strains, for definition of balancers). Over-expressing *PHM* in a wild-type background (Table 4, lines 4 and 5) did not degrade behavioral rhythmicity. By both periodogram and SNR analysis, most control strains appeared less rhythmic than wild-type animals but considerably more rhythmic than *per*^{01} or *pdf*^{01} (Fig. 6*A*, Table 4). Of the six control combinations tested, two displayed less rhythmicity than the others. Line 6 (*y w*; *c929-gal4*/UAS:*PHM*, *PHM*^{02}) produced a nominally lower percentage of rhythmic animals by periodogram analysis, but also displayed a moderately high SNR average (0.95). Line 7 (*y w*; *c929-gal4*, *PHM*$^{[01]}$/*y*$^{+}$, *CyO*) produced a lower average SNR, but 77% were rhythmic by periodogram.

The effect of combining different *gal4* elements on LD behavior

We combined *gal4* elements with *36Y-gal4* or *c929-gal4* to try and improve behavior displayed by animals rescued with either *gal4* element alone. D42-*gal4* was used because it provides a modest increase in the spatial patterns provided by the *36Y*- and *c929-gal4* elements, specifically by including most motorneurons (G. Boulianne, personal communication). *Appl*(3GK)-*gal4*, c155(*elav*)-*gal4* and *tim-gal4* were used to effect widespread (i.e., most or all CNS) expression. Finally, *pdf-gal4* (two distinct lines, called M and N) ensured expression of PHM in all LN-Vs (these neurons secrete the amidated peptide PDF). Combining *36Y-gal4*, D42-*gal4*, or *pdf*(M)-*gal4* with *c929-gal4* produced LD behavior that was aberrant and similar to that of *c929-gal4* alone (Fig. 6). Combining *pdf*(N)-*gal4*, *Appl-gal4*, c155-*gal4*, *386Y-gal4*, or *tim*-

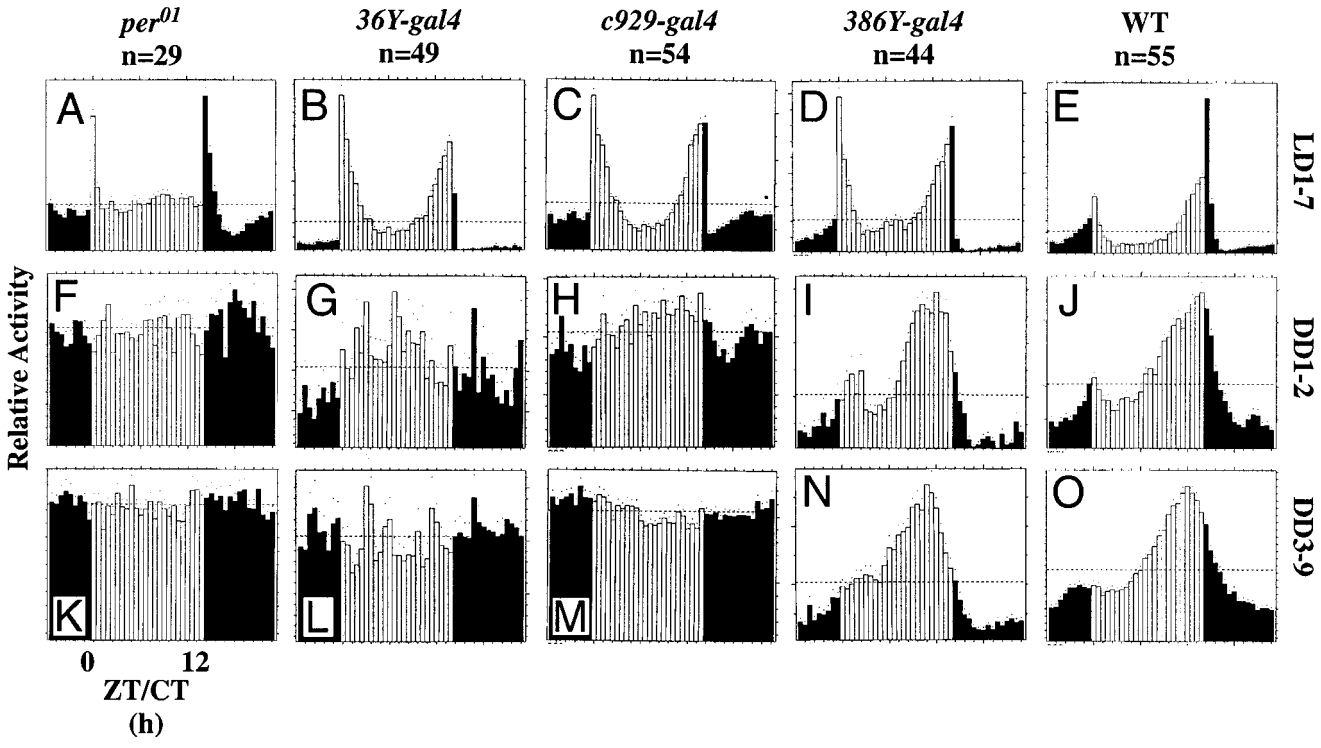

Figure 4. Locomotor activity of normal, per^0, and single *gal4:*UAS-*PHM*-rescued *PHM* mutant flies. Average activity histograms indicating relative levels of locomotion. *White* and *black bars* indicate the day and night phases in LD, respectively (Hamblen-Coyle et al., 1989, 1992). *n*, number of flies tested. For the constant dark (*DD*) plots (*rows 2* and *3*), *white bars* designate the subjective day. *Dots* indicate SEM values for that 30 min time bin with reference to average level of activity per fly. *A*, *F*, *K*, per^{01}; *B*, *G*, *L*, *36Y-gal4:*UAS-*PHM*-rescued *PHM* mosaics; *C*, *H*, *M*, *c929-gal4:*UAS-*PHM*-rescued *PHM* mosaics; *D*, *I*, *N*, *386Y-gal4:*UAS-*PHM*-rescued *PHM* mosaics; *E*, *J*, *O*, Canton-S wild type. *A–E*, 7 d of LD behavior; *F–J*, behavior during DD days 1–2; *K–O*, behavior during DD days 3–9. *ZT*, Zeitgeber time; *CT*, circadian time.

gal4 with *c929-gal4* produced LD behavior that resembled that of control stocks (Figs. 7, 8*B*,*C*). Finally, combining *tim-gal4* with *36Y-gal4* produced LD behavior that resembled that of control stocks (Fig. 8*A*).

The effect of combining different *gal4* elements on DD behavior

Weak rhythmicity in DD was produced in three combinations of *gal4* elements. Combining *36Y-gal4*, D42-*gal4*, or *pdf*(M)-*gal4* with *c929-gal4* did not improve the performance of animals beyond that of *c929-gal4* alone (Fig. 6*G--I*, Table 4). Combining *Appl*(3GK)-*gal4* with *c929-gal4* increased the percentage of rhythmic individuals (to 48%), but the group retained a low average SNR (0.49) (Fig. 7*H*, Table 4). Likewise, combining *pdf*(N)-*gal4* with *c929-gal4* also increased the percentage of rhythmic flies (to 43%), yet the average SNR remained low (0.55) (Fig. 7*G*, Table 4). The same was true for combining c155-*gal4* with *c929-gal4*; by periodogram analysis, 72% of these animals were rhythmic, yet they retained a low average SNR (0.48) (Fig. 7*I*, Table 4).

Strong rhythmicity in DD was produced in three combinations of *gal4* elements. Combining *tim-gal4* with *36Y-gal4* produced 84% rhythmic individuals and a markedly higher average SNR (0.89) than displayed by *36Y-gal*4 alone (Fig. 8*G*, Table 4, compare lines 11 and 16). Combining *tim-gal4* with *c929-gal4* also increased the percentage of rhythmic flies (to 84%) and moderately improved the average SNR (0.76) (Fig. 8*I*, Table 4, compare lines 12 and 20). Combining *386Y-gal4* with *c929-gal4* produced DD behavior that resembled animals bearing only *386Y-gal4* (Fig. 8*H*, Table 4, compare lines 10 and 16). By MESA, the periods displayed under constant conditions were not significantly different, with the exception of animals containing the *36Y-gal4* element (Table 4).

The distribution of SNR values in animals in which *c929-gal4* was combined with either *36Y-gal4*, D42-*gal4*, or *pdf*(M)-*gal4* confirmed the hypothesis that none of these combinations significantly improved the rhythmicity of *c929-gal4*-rescued animals (Fig. 9*A*). Likewise, adding *pdf*(N)-*gal4*, c155-*gal4*, or Appl-*gal4* to *c929-gal4* produced only a moderate improvement in the distribution of SNR values (Fig. 9*B*). Both sets of distributions were heavily weighted in the range 0.3–0.5. In contrast, the combination of *c929-gal4* with *386Y-gal4* produced a distribution that resembled that of *386Y-gal4*-rescued flies alone (Fig. 9*C*). Likewise, combining *tim-gal4* with either *36Y-gal4* or *c929-gal4* produced balanced SNR distributions that more resembled that of WT (Fig. 9*C*). Table 4 includes the results of statistical analysis comparing each DD days 3–9 SNR data set with that of the *c929-gal4*-rescued population.

Lack of correlation between average activity levels and rhythmicity

We asked whether the average activity levels of different genotypes in DD days 3–9 predicted the strength of behavioral rhythmicity (Table 4). In general, these traits did not appear strongly correlated. Some, but not all, rescued lines displayed normal activity levels. For example, *36Y-gal4*-rescued flies displayed the lowest levels of average activity under constant conditions, and this was in accord with their weak rhythmicity (Table 4, genotype 11). However, although the level of activity of *36Y-gal4*-rescued animals was not markedly improved by the addition of *tim-gal4*, that double transgenic combination (*36Y-gal4* and *tim(#16)-gal4*)

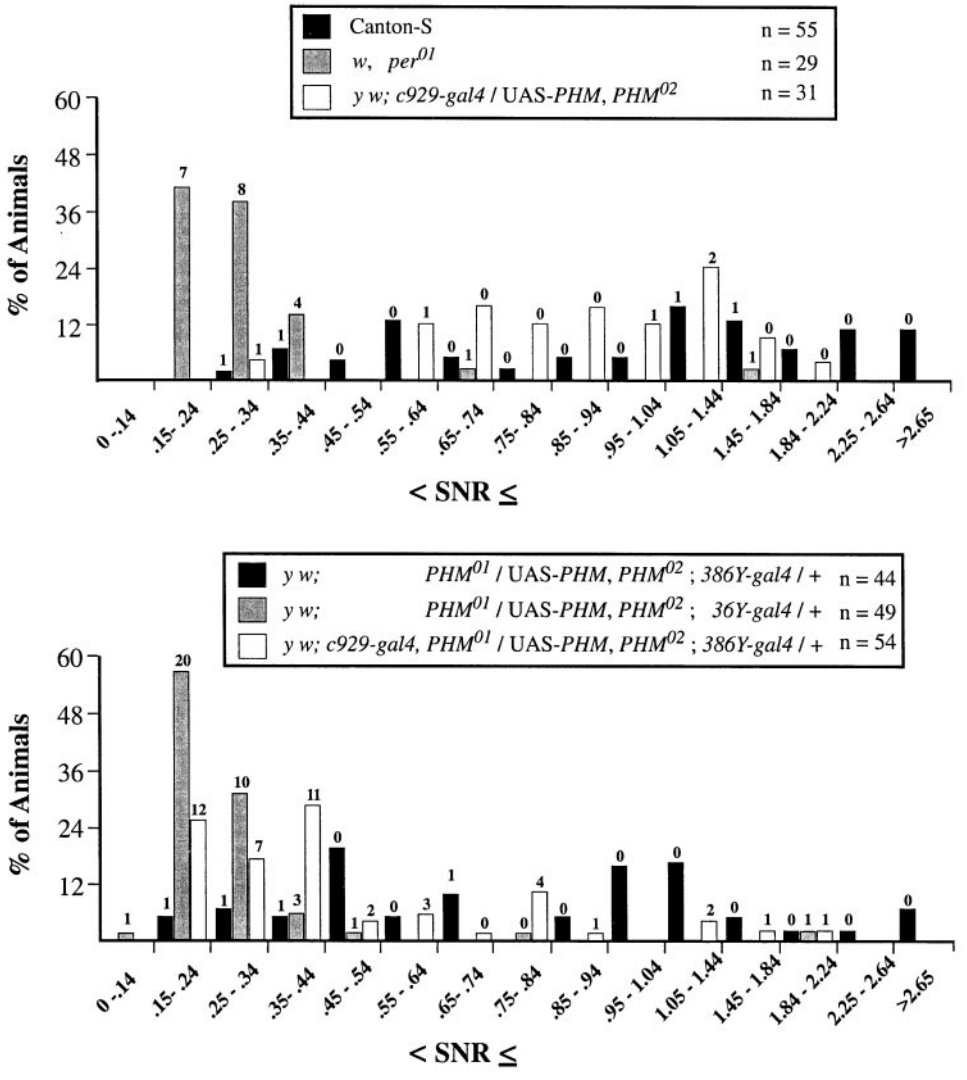

Figure 5. Numerical measures of varying behavioral rhythm strengths in per^{01}, normal, and single *gal4*-rescued *PHM* mutants. Signal-to-noise ratios (*SNR*s) for the final 7 d (DD days 3–9) of the free running period (see Table 4). The *panels* indicate SNR distributions for per^{01}, *y w*; *c929-gal4*/UAS-*PHM*, PHM^{02}, and Canton-S (*top*); and *y w*; PHM^{01}/UAS-*PHM*, PHM^{02} containing either *36Y-gal4*, *c929-gal4*, or *386Y-gal4* (*bottom*). SNR values ≤1.04 were divided into increments of 0.1; between 1.05 and 2.64, SNR values were divided into increments of 0.3; all SNR values >2.65 were grouped together. The *ordinate values* are the percentage of total flies whose SNR falls within each interval. The *numbers* of flies that were scored arrhythmic by χ-square periodogram analysis are indicated *above* the histogram bars. For the rhythmic individuals, free-running periods of the different genotypes were calculated by Maximum Entropy Spectral Analyses independently of those in Table 4; they were not significantly different by ANOVA (means: Canton-S, 24.1 ± 0.2 hr; per^{01}, 24.9 ± 1.2 hr; *y w;* PHM^{01}/UAS-*PHM*, PHM^{02}; *386Y-gal4*/+, 23.4 ± 0.3 hr; *y w*; PHM^{01}/UAS-*PHM*, PHM^{02}; *36Y-gal4*/+, 23.9 ± 0.8 hr; *y w*; *c929-gal4*/UAS-*PHM*, PHM^{02}, 23.8 ± 1.1 hr).

produced strong rhythmicity by both periodogram and SNR analysis (Table 4, genotype 20). Likewise, *386Y-gal4*-rescued flies produced strong measures of rhythmicity in DD days 3–9, yet also displayed low levels of average activity (Table 4, genotype 10).

DISCUSSION

We used a genetic approach to create animal mosaics for PHM, a biosynthetic enzyme that is required for maturation of the majority of neuropeptide transmitters in *Drosophila* (Jiang et al., 2000). By studying their behavior, we draw two principal conclusions. First, PHM enzyme activity, and hence C-terminal amidation of peptide transmitters, is required for normal circadian locomotion in *Drosophila*. Second, amidated neuropeptides, in addition to PDF, are required to regulate circuits controlling this behavior.

Neuropeptide amidation is required for daily locomotor rhythms

Our results support the hypothesis that daily locomotor rhythms in flies require signaling by neuropeptides that are C-terminally amidated. We first showed that the *gal4*/*UAS-PHM* system predictably controls PHM spatial expression. Next, we found that certain PHM mosaic flies (e.g., *36Y-gal4*- and *c929-gal4*-rescued) were largely arrhythmic under conditions of constant darkness. Our working hypothesis is that such a behavioral disruption is attributable to changes in the normal patterns of peptide amidation. We have not demonstrated the last point directly. It is a premise based on the previous demonstration that manipulation of PHM produces large-scale changes in peptide amidation in both larval and adult stages (Jiang et al., 2000).

A second result supports the conclusion that amidated peptides contribute to daily locomotor rhythms; increasing *PHM* expression by combining *pdf*(N)-*gal4* with *c929-gal4* improved rhythmic behavior over that displayed by *c929-gal4* alone. Although the combination did not completely restore wild-type behavior, the improvement indicates that PHM activity in PDF neurons does contribute to display of rhythmic daily locomotion. We presume that this indicates a requirement for amidation of PDF because the pigment-dispersing activity of PDH on crustacean melanophores is highly dependent (~300-fold) on the C-terminal amide (Riehm et al., 1985). Whether PDF must be modified as such to display circadian signaling activity is unknown.

Neuropeptides besides PDF are required for daily locomotor rhythms

The strongest evidence for this conclusion comes from the performance of *36Y-gal4*- and *c929-gal4*-rescued flies under constant

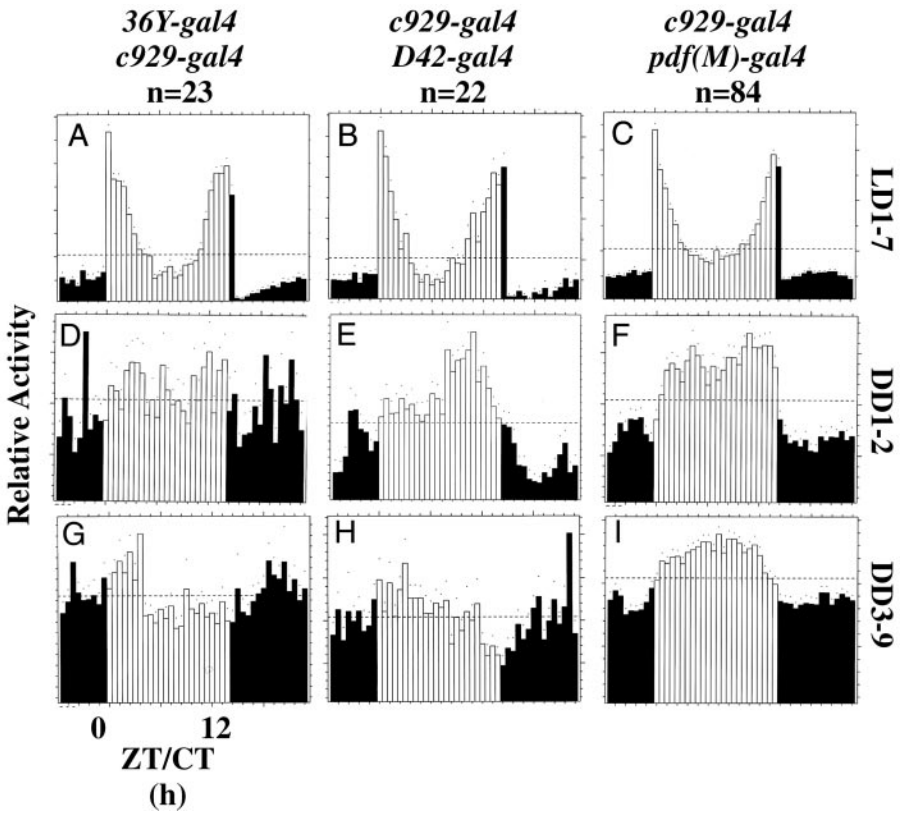

Figure 6. Locomotor activity of double *gal4:*UAS-*PHM*-rescued *PHM* mutant flies. Average activity histograms for groups of flies, plotted as described in Figure 4. *n*, number of flies tested. *A*, *D*, *G*, *36Y-gal4*/*c929-gal4:*UAS-*PHM*-rescued *PHM* mosaics; *B*, *E*, *H*, *c929-gal4*/*D42-gal4:*UAS-*PHM*-rescued *PHM* mosaics; *C*, *F*, *I*, *c929-gal4*/*pdf*(*M*)*-gal4:*UAS-*PHM*-rescued *PHM* mosaics.

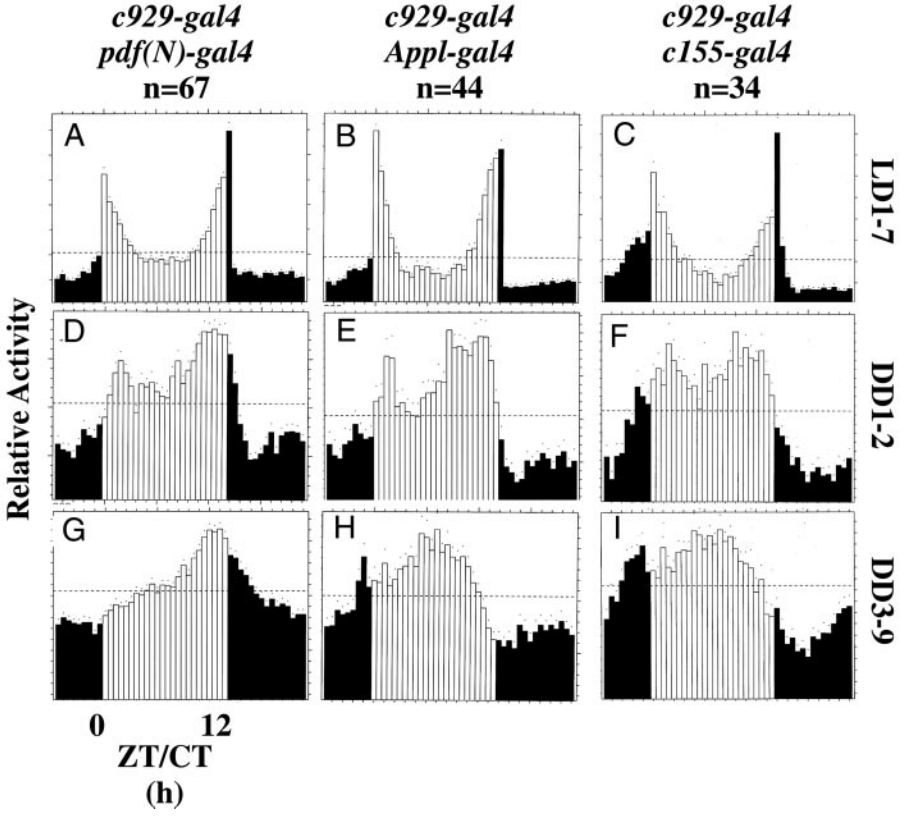

Figure 7. Locomotor activity of double *gal4:*UAS-*PHM*-rescued *PHM* mutant flies. Average activity histograms for groups of flies, plotted as described in Figure 4. *n*, number of flies tested. *A*, *D*, *G*, *c929-gal4*/*pdf*(*N*)*-gal4:*UAS-*PHM*-rescued *PHM* mosaics; *B*, *E*, *H*, *c929-gal4*/*Appl-gal4:*UAS-*PHM*-rescued *PHM* mosaics; *C*, *F*, *I*, *c929-gal4*/c155-*gal4:*UAS-*PHM*-rescued *PHM* mosaics.

conditions. Unlike pdf^{01} flies, these populations displayed little rhythmicity behavior during the first cycle of constant conditions (cf. Renn et al., 1999). Also, the average SNR of *36Y-gal4*-rescued flies was much less than that of pdf^{01} and very comparable with that of per^{01}. Are such deficits attributable to a loss of *PHM* function or a gain of deleterious function? The *pdf* neuropeptide gene can produce a gain-of-function phenotype: When *pdf* was misexpressed by certain *gal4* drivers in WT flies, rhythmic loco-

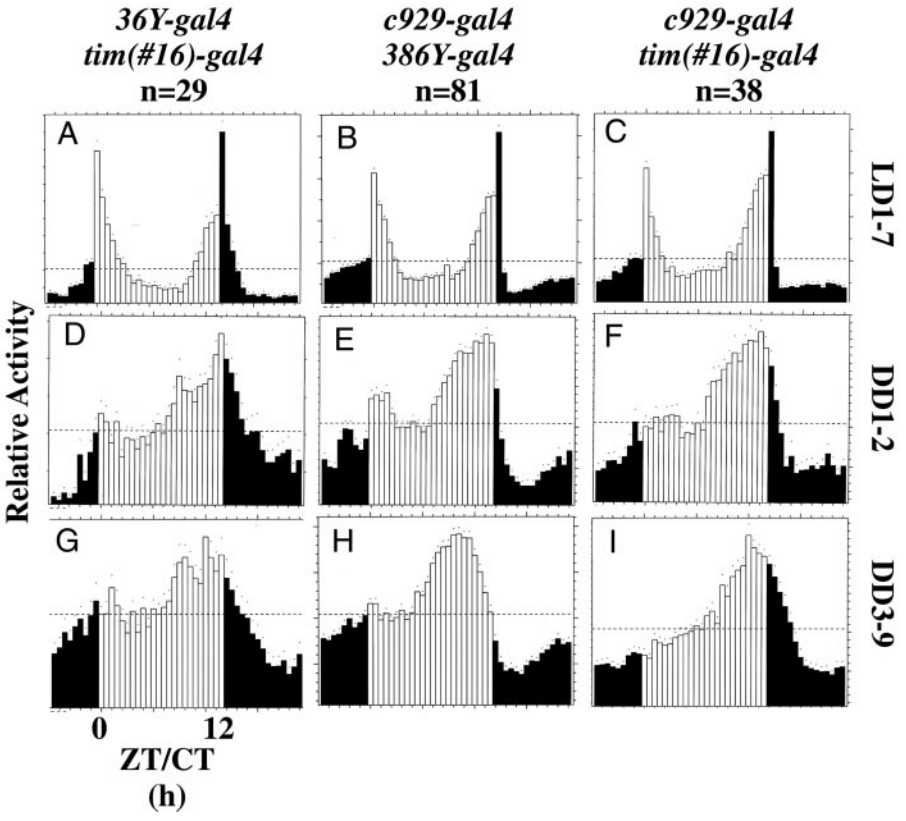

Figure 8. Locomotor activity of double *gal4:*UAS-*PHM*-rescued *PHM* mutant flies. Average activity histograms for groups of flies, plotted as described in Figure 4. *n*, number of flies tested. *A*, *D*, *G*, *36Y-gal4*/*tim(#*16)-*gal4:*UAS-*PHM*-rescued *PHM* mosaics; *B*, *E*, *H*, *c929-gal4*/*386Y-gal4:*UAS-*PHM*-rescued *PHM* mosaics; *C*, *F*, *I*, *c929-gal4*/*tim(#*16)-*gal4:*UAS-*PHM*-rescued *PHM* mosaics.

motor behavior was degraded (Helfrich-Förster et al., 2000). In the case of *PHM*, however, two results suggest it is the absence of the enzyme that causes arrhythmicity. First, increasing *PHM* expression (by adding *tim-gal4* to *36Y-gal4* or *c929-gal4*) restored near-normal rhythmicity to both arrhythmic lines. Second, misexpression of *PHM* by driving it with *tim-gal4* or with *c929-gal4* in a WT did not degrade behavioral rhythmicity. In general, the greater the extent of *PHM* gene expression in a *PHM* mutant background, the more predictable was the degree of behavioral improvement. Interestingly, some combinations restored considerable *PHM* expression (e.g., *Appl-gal4*) but improved behavioral performance only moderately. Together, those experiments suggest that normal *PHM* expression is required in specific neurons and/or secretory cells for the behavior examined. The *tim-gal4* line produced a broad expression pattern of great complexity. That amount of expression precludes clear definition of places or times by which "additional" PHM restored the functions of circadian regulatory circuits. This point is discussed further in the next section.

Interpretation of *gal4* expression patterns

We compared the behavior of stocks that each contained multiple transposons. To improve the scope of the study, we tested five control genotypes that combined subsets of the multiple transposons used in the experimental genotypes. In general, these controls displayed a level of rhythmicity lower than that of WT but greater than those of *PHM* mosaics (Table 4). *gal4* lines are used primarily to create spatial differences in gene expression (Helfrich-Förster et al., 2000; Waddell et al., 2000). We chose three *gal4* lines for this study (*36Y*, *c929*, and *386Y*), because their expression patterns prominently featured peptidergic neurons of the CNS and secretory cells of peripheral tissues. The three patterns were very similar; the fact that all successfully reverted *PHM* lethality (Table 2) is probably a reflection of such anatomical similarities. The *gal4* patterns also included clear differences in cell number (*386Y* > *c929* > *36Y*).

These pattern differences are of interest, because they may reveal specific neurons (or non-neuronal cells) that produce secretory peptides required for circadian behaviors. However, we concluded that the interpretation of where "critical *PHM* expression" occurs in these experiments is problematic, because there are several ways by which such patterns may defy simple interpretation. For example, two *gal4* patterns could appear similar and stable in the adult stage, yet be different because of a transient event during development. In fact, the *c929-gal4* pattern is relatively stable in the adult stage but transiently includes the VA neuroendocrine neurons (O'Brien and Taghert, 1998) for only a brief period during adult development (P. H. Taghert, unpublished observations). In such a case, behavioral rescue may reflect temporal, not spatial, differences in *gal4*-dependent gene expression. A separate problem in the interpretation could arise when two patterns are spatially similar but differ in levels of expression by specific neurons. In that case, the extent of behavioral rescue may reflect quantitative, not spatial, differences in *gal4*-dependent gene expression.

Given these complexities, we are currently unable to specify in which neurons, beyond the LN-V, PHM activity is required for daily locomotor rhythms. Instead, for subsequent analysis we favor considering candidate amidated neuropeptides directly. From scans of the *Drosophila* genome, there are at least 23 neuropeptide-encoding genes (Hewes and Taghert, 2001; Vanden Broeck, 2001): This is likely an underestimate because

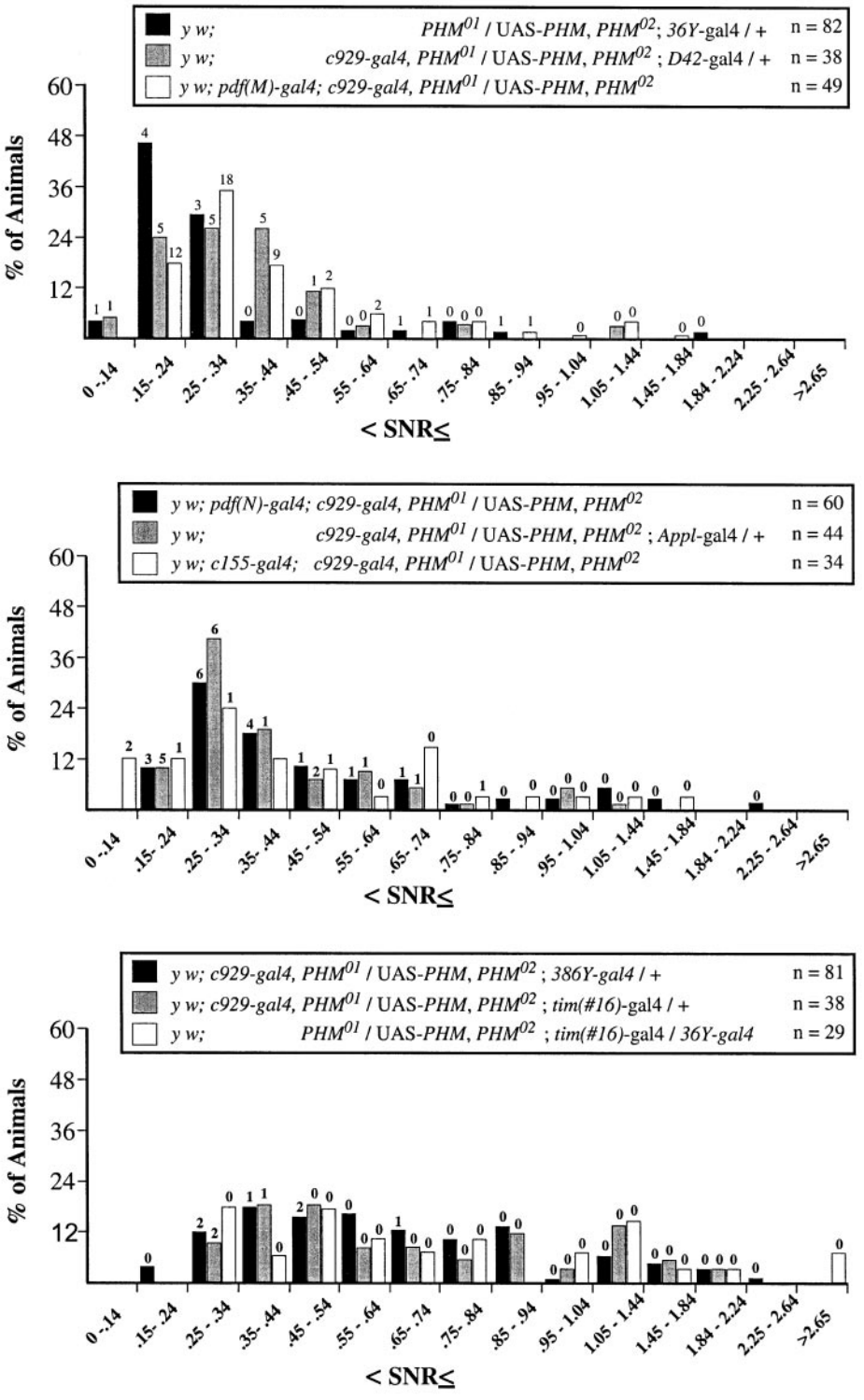

Figure 9. Numerical measures of varying behavioral rhythm strengths in double *gal4*-rescued *PHM* mutant flies. SNR values for the final 7 d (DD days 3–9) of the free running period presented as described in Figure 5. The *panels* indicate SNR distributions for *y w*; *PHM*^{01}/UAS-*PHM, PHM*^{02} containing either *c929-gal4* and *36Y-gal4*, *c929-gal4* and *D42-gal4*, or *c929-gal4* and *pdf*(*M*)*-gal4* (*top*); *y w*; *PHM*^{01}/UAS-*PHM, PHM*^{02} containing either *c929-gal4* and *pdf*(*N*)*-gal4*, *c929-gal4* and *Appl-gal4*, or *c929-gal4* and c155-*gal4* (*middle*); and *y w*; *PHM*^{01}/UAS-*PHM, PHM*^{02} containing either *c929-gal4* and *386Y-gal4*, *c929-gal4* and *tim*(#16)*-gal4*, or *36Y-gal4* and *tim*(*#16*)*-gal4* (*bottom*). The *ordinate values* are the percentage of total flies whose SNR falls within each interval. The *numbers* of flies that were scored arrhythmic by χ-square periodogram analysis are indicated *above* the histogram bars. For the rhythmic individuals, free-running periods of the different genotypes were calculated by Maximum Entropy Spectral Analyses, independently of those in Table 4; they were not significantly different by ANOVA (means = *y w*; *c929-gal4*, *PHM*^{01}/UAS-*PHM, PHM*^{02}; *36Y-gal4*/ +, 25.4 ± 1.5 hr; *y w*, *pdf-gal4*(M); *y w*; *c929-gal4*/UAS-*PHM*, *PHM*^{02}, 24.4 ± 0.4 hr; *y w*; *c929-gal4*, *PHM*^{01}/ UAS-*PHM, PHM*^{02}; *D42-gal4*/ +, 24.2 ± 1.0 hr; *y w*, *pdf-gal4*(N); *c929-gal4*, *PHM*^{01}/ UAS-*PHM, PHM*^{02}, 25.2 ± 0.3 hr; *y w*; *c929-gal4*, *PHM*^{01}/ UAS-*PHM, PHM*^{02}; *Appl3GK-gal4*/ +, 24.0 ± 0.4 hr; *y w*; *c929-gal4* and c155-*gal4*, 24.1 ± 0.6 hr; *y w*; *c929-gal4*, *PHM*^{01}/UAS-*PHM, PHM*^{02}; *386Y-gal4*/+, 24.1 ± 0.3 hr; *y w*; *c929-gal4*, *PHM*^{01}/ UAS-*PHM, PHM*^{02}; *tim(#16)-gal4*/ +, 24.0 ± 0.2 hr; *y w*; *PHM*^{01}/UAS-*PHM, PHM*^{02}; *tim(#16)-gal4*/ *36Y-gal4*, 24.9 ± 0.4 hr).

of the difficulty in predicting neuropeptide precursor sequences with accuracy. Of the identified genes, ~20 encode peptides that are known or are predicted to display C-terminal amidation. Thus, it may be reasonable to systematically address the roles of each of the ~20 precursors using *Drosophila* genetics.

General activity versus the circadian organization of activity in *PHM* mosaics

Genetic studies of circadian behaviors traditionally strive to establish that a mutant phenotype does not simply degrade the ability to produce movement (Hamblen-Coyle et al., 1989). Here,

we analyzed the behavior of animals with large-scale alterations in transmitter profiles throughout the entire nervous system. In one genotype (*36Y-gal4/UAS-PHM*), rhythmicity under constant conditions was extremely poor (as low as that of per^{01} animals); activity levels were also lower than in other genotypes tested. Nevertheless, when the locomotor rhythm of *36Y-gal4*-rescued animals was restored by addition of *tim-gal4*, activity levels were not also increased. We propose that the *36Y-gal4* transmitter mosaic contains disruptions of distinct neural centers, ones that control the general level of activity and ones that organize rest–activity cycles. A similar point is made considering the results seen with *tim-gal4*. Addition of *tim-gal4* to *36Y-gal4*-rescued flies produced the greatest restoration of rhythmicity. However, *tim-gal4* was by itself unable to revert the lethality of *PHM* mutants. Therefore, places and times of *PHM* expression that promote normal vitality do not necessarily equal those promoting circadian behavioral rhythmicity.

The behavior of these PHM mosaics differed from that of clock gene mutants

Flies lacking clock gene function (e.g., per^{0}) (Wheeler et al., 1993) display light-driven behavior under cycling conditions (Fig. 4*A*), then become arrhythmic during the first cycle of constant conditions (Fig. 4*F*). Arrhythmic *PHM* mosaics were different. For example, *36Y-gal4*-rescued flies, whose rhythmicity under constant conditions was quantitatively as weak as that of per^{01} animals, entrained well during LD. Therefore, we conclude that even the most severely arrhythmic *PHM* mosaic animals we have studied have levels of circadian clock function and output greater than that present in authentic clock mutants.

Evidence for graded levels of rhythmic behavior

The average activity histograms for behavior under constant conditions indicated that different *gal4* drivers produced graded levels in circadian locomotor performance. We found evidence for at least three levels. The lowest level was represented by single *gal4* flies (e.g., *36Y*); they had the weakest measures of rhythmicity (by periodogram or MESA) and displayed little reproducible variation in the average activity histogram. An intermediate level was seen in certain *gal4*-combination flies (e.g., *c929/D42*); these displayed moderate rhythmicity and an average activity peak during early subjective day. The strongest level was seen in other *gal4*-combination flies (e.g., *c929/tim*); these were strongly rhythmic, and they displayed a large average activity peak during late subjective day and a rapid decrease in activity during early subjective night. Presumably, these graded levels of performance reflect incremental contributions by different amidated peptides to one or more circuit components. Relating specific peptide systems to separate levels of behavioral performance represents a challenge for future studies.

REFERENCES

Aasland R, Gibson TJ, Stewart AF (1995) The PHD finger: implications for chromatin-mediated transcriptional regulation. Trends Biochem Sci 20:56–59.

Benveniste RJ, Taghert PH (1999) Cell type-specific regulatory sequences control expression of the *Drosophila FMRF-NH$_2$* neuropeptide gene. J Neurobiol 38:507–520.

Brand AH, Perrimon N (1993) Targeted gene expression as a means of altering cell fates and generating dominant phenotypes. Development 118:401–415.

Dowse HB, Ringo JM (1987) Further evidence that the circadian clock in *Drosophila* is a population of coupled ultradian period. J Biol Rhythms 2:65–76.

Dushay MS, Rosbash M, Hall JC (1989) The *disconnected* visual system mutations in *Drosophila melanogaster* drastically disrupt circadian rhythms. J Biol Rhythms 4:1–27.

Eipper BA, Stoffers DA, Mains RE (1993) Biosynthesis of neuropeptides: alpha-amidation. Annu Rev Neurosci 15:57–85.

Ewer J, Frisch B, Hamblen-Coyle MJ, Rosbash M, Hall JC (1992) Expression of the *period* clock gene within different cell types in the brain of *Drosophila* adults and mosaic analysis of these cells' influence on circadian behavioral rhythms. J Neurosci 12:3321–3349.

Frisch B, Hardin PE, Hamblen-Coyle MJ, Rosbash M, Hall JC (1994) A promoterless *period* gene mediates behavioral rhythmicity and cyclical *per* expression in a restricted subset of the *Drosophila* nervous system. Neuron 12:555–570.

Gloor GB, Preston CR, Johnson-Schlitz DM, Nassif NA, Phillis RW, Benz WK, Robertson HM, Engels WR (1993) Type I repressors of P-element mobility. Genetics 135:81–95.

Hamblen MJ, Zehring WA, Kyriacou CP, Reddy P, Yu Q, Wheeler DA, Zweibel LJ, Konopka RJ, Rosbash M, Hall JC (1986) Germ-line transformation involving DNA from the *period* locus in *Drosophila melanogaster*: overlapping genomic fragments that restore circadian and ultradian rhythmicity to per^{0} and per^{-} mutants. J Neurogenet 3:249–291.

Hamblen MJ, White NE, Emery PT, Kaiser K, Hall JC (1998) Molecular and behavioral analysis of four *period* mutants in *Drosophila melanogaster* encompassing extreme short, novel long, and unorthodox arrhythmic types. Genetics 149:165–178.

Hamblen-Coyle M, Konopka RJ, Zwiebel LJ, Colot HV, Dowse HB, Rosbash M, Hall JC (1989) A new mutation at the *period* locus of *Drosophila melanogaster* with some novel effects on circadian rhythms. J Neurogenet 5:229–256.

Hamblen-Coyle MJ, Wheeler DA, Rutila JE, Rosbash M, Hall JC (1992) Behavior of period-altered circadian rhythm mutants of *Drosophila* in light:dark cycles (Diptera: *Drosophilidae*). J Insect Behav 5:417–446.

Helfrich-Förster C (1995) The *period* clock gene is expressed in central nervous system neurons which also produce a neuropeptide that reveals the projections of circadian pacemaker cells within the brain of *Drosophila melanogaster*. Proc Natl Acad Sci USA 92:612–616.

Helfrich-Förster C (1998) Robust circadian rhythmicity of *Drosophila melanogaster* requires the presence of lateral neurons: a brain-behavioral study of disconnected mutants. J Comp Physiol [A] 182:435–453.

Helfrich-Förster C, Tauber M, Park JH, Muhlig-Versen M, Schneuwly S, Hofbauer A (2000) Ectopic expression of the neuropeptide pigment-dispersing factor alters behavioral rhythms in *Drosophila melanogaster*. J Neurosci 20:3339–3353.

Hewes RS, Taghert PH (2001) Neuropeptides and neuropeptide receptors in the *Drosophila melanogaster* genome. Genome Res 11:1126–1142.

Hewes RS, Schaefer AM, Taghert PH (2000) The *cryptocephal* gene (*ATF4*) encodes multiple basic-leucine zipper proteins controlling molting and metamorphosis in *Drosophila*. Genetics 155:1711–1723.

Jiang N, Kolhekar AS, Jacobs PS, Mains RE, Eipper BA, Taghert PH (2000) *PHM* is required for normal developmental transitions and for biosynthesis of secretory peptides in *Drosophila*. Dev Biol 226:118–136.

Kaneko M, Hall JC (2000) Neuroanatomy of cells expressing clock genes in *Drosophila*: transgenic manipulation of the *period* and *timeless* genes to mark the perikarya of circadian pacemaker neurons and their projections. J Comp Neurol 422:66–94.

Kolhekar AS, Roberts MS, Jiang N, Johnson RC, Mains RE, Eipper BA, Taghert PH (1997) Neuropeptide amidation in *Drosophila*: separate genes encode the two enzymes catalyzing amidation. J Neurosci 17:1363–1376.

Lin DM, Goodman CS (1994) Ectopic and increased expression of Fasciclin II alters motoneuron growth cone guidance. Neuron 13:507–523.

Majercak J, Sidote D, Hardin PE, Edery I (1999) How a circadian clock adapts to seasonal decreases in temperature and day length. Neuron 24:219–230.

Maniatis T, Fritsch EF, Sambrook J (1982) Molecular cloning: a laboratory manual. Cold Spring Harbor, NY: Cold Spring Harbor Laboratory.

O'Brien MA, Taghert PH (1998) A peritracheal neuropeptide system in insects: release of myomodulin-like peptides at ecdysis. J Exp Biol 201:193–209.

O'Brien MA, Schneider LE, Taghert PH (1991) *In situ* hybridization analysis of the *FMRFamide* neuropeptide gene in *Drosophila*. II. Constancy in the cellular pattern of expression during metamorphosis. J Comp Neurol 304:623–638.

Park JA, Helfrich-Förster C, Lee G, Liu L, Rosbash M, Hall JC (2000) Differential regulation of circadian pacemaker output by separate clock genes in *Drosophila*. Proc Natl Acad Sci USA 97:3608–3613.

Riehm JP, Rao KR, Semmes OJ, Jorenby WH, Hintz MF, Zahnow CA (1985) C-terminal deletion analogs of a crustacean pigment-dispersing hormone. Peptides 6:1051–1056.

Renn SCP, Park JH, Rosbash M, Hall JC, Taghert PH (1999) A *pdf* neuropeptide gene mutation and ablation of PDF neurons both cause

severe abnormalities of circadian behavioral rhythms in *Drosophila*. Cell 99:791–802.

Siekhaus DE, Fuller RS (1999) A role for *amontillado*, the *Drosophila*-homolog of the neuropeptide precursor processing protease PC2, in triggering hatching behavior. J Neurosci 19:6942–6954.

Silver R, LeSauter J, Tresco PA, Lehman MN (1996) A diffusible coupling signal from the transplanted suprachiasmatic nucleus controlling circadian locomotor rhythms. Nature 382:810–813.

Silver R, Sookhoo AI, LeSauter J, Stevens P, Jansen HT, Lehman MN (1999) Multiple regulatory elements result in regional specificity in circadian rhythms of neuropeptide expression in mouse SCN. NeuroReport 10:3165–3174.

Sokolove PG, Bushell WN (1978) The χ-square periodogram: its utility for analysis of circadian rhythms. J Theor Biol 72:131–160.

Taghert PH, Schneider LE (1990) Inter-specific comparison of a *Drosophila* gene encoding FMRFamide-related neuropeptides. J Neurosci 10:1929–1942.

Vanden Broeck J (2001) Neuropeptides and their precursors in the fruitfly, *Drosophila melanogaster*. Peptides 22:241–254.

Waddell S, Armstrong JD, Kitamoto T, Kaiser K, Quinn WG (2000) The *amnesiac* gene product is expressed in two neurons in the *Drosophila* brain that are critical for memory. Cell 103:805–813.

Wheeler DA, Hamblen-Coyle MJ, Dushay MS, Hall JC (1993) Behavior in light-dark cycles of *Drosophila* mutants that are arrhythmic, blind, or both. J Biol Rhythms 8:67–94.

Zitnan D, Kingan TG, Hermesman JL, Adams ME (1996) Identification of ecdysis-triggering hormone from an epitracheal endocrine system. Science 271:88–91.